Numerical and experimental study on coherent beam combining of fibre amplifiers using simulated annealing algorithm

Zhou Pu(周 朴), Ma Yan-Xing (马阎星), Wang Xiao-Lin(王小林),
Ma Hao-Tong(马浩统), Xu Xiao-Jun(许晓军), and Liu Ze-Jin(刘泽金)†

College of Optoelectric Science and Engineering, National University of Defense Technology, Changsha 410073, *China*

(Received 3 May 2009; revised manuscript received 31 August 2009)

We present the numerical and experimental study on the coherent beam combining of fibre amplifiers by means of simulated annealing (SA) algorithm. The feasibility is validated by the Monte Carlo simulation of correcting static phase distortion using SA algorithm. The performance of SA algorithm under time-varying phase noise is numerically studied by dynamic simulation. It is revealed that the influence of phase noise on the performance of SA algorithm gets stronger with an increase in amplitude or frequency of phase noise; and the laser array that contains more lasers will be more affected from phase noise. The performance of SA algorithm for coherent beam combining is also compared with a widely used stochastic optimization algorithm, i.e., the stochastic parallel gradient descent (SPGD) algorithm. In a proof-of-concept experiment we demonstrate the coherent beam combining of two 1083 nm fibre amplifiers with a total output power of 12 W and 93% combining efficiency. The contrast of the far-field coherently combined beam profiles is calculated to be as high as 95%.

Keywords: coherent beam combining, simulated annealing, laser array, stochastic parallel gradient descent

PACC: 4225K, 4255N, 4260F

1. Introduction

The coherent beam combining of fibre lasers/amplifiers has been under intensive research recently.[1−12] As a promising technique, coherent beam combining based on stochastic optimization algorithm is of great potential for their advantage of less complexity while maintaining the capability in scaling to a large number of beamlets. In previous work, coherent beam combining based on stochastic parallel gradient descent (SPGD) algorithm (a kind of stochastic optimization algorithm) has been demonstrated by Liu[10] and Kansky.[11] Our group has also demonstrated coherent beam combining of three W-level fibre amplifiers.[12]

Another kind of stochastic optimization algorithm that has been used gradually in optical technology area is the simulated annealing (SA) algorithm. Theoretical work and initial simulations have shown that the optical problem can be transformed into a model for crystal roughening that served as a motivation to implement the SA algorithm.[13] The first hardware realization of the SA algorithm in an adaptive optics system was realized by Zommer[14] in 2006, and it was shown that the SA algorithm may have good results in converging into global extremum in simulations. Coherent beam combining of fibre lasers can be considered as the piston-type phase aberration compensating in the adaptive optics system, so it is seen straightforwardly that the SA algorithm has the potential to be used for coherent beam combining. To the best of our knowledge, the application of the SA algorithm in coherent beam combining has not been reported yet.

In this paper, we will present our numerical and experimental study on coherent beam combining using the SA algorithm. This paper is organized as follows: in Section 2, we present a brief introduction to SA algorithm. In Section 3, we give the system setup and technique details for coherent beam combining using the SA algorithm; the feasibility of coherent beam combining using the SA algorithm will be validated by correcting static phase aberrations with SA algorithm. For a more general case, the performance of co-

†Corresponding author. E-mail: zejinliu@vip.sina.com

© 2010 Chinese Physical Society and IOP Publishing Ltd

herent beam combining using the SA algorithm when dynamic phase noise exists is simulated and analysed in Section 4. As a proof-of-concept experiment, we will present the experimental study on coherent beam combining of two fibre amplifiers with a total output power of 12 W using the SA algorithm in Section 5. The summary will be given in Section 6.

2. Brief introductions to SA algorithm[14,15]

In the SA algorithm, the term annealing comes from analogies to the cooling of a liquid or solid. A central issue in statistical mechanics is to analyse the behaviour of substances as they cool. At high temperatures, molecules or atoms have much mobility, but as the temperature decreases to a certain value, this mobility will be lost and the molecules or atoms tend to align themselves in a crystalline structure. This aligned structure is the minimum energy state of the system. To achieve this state, the cooling must be carried out at a sufficiently slow rate. The principle behind annealing in physical systems is the slow cooling of substances to reach the minimum energy state. In optimization, the analogy to a minimum energy state for a system is a minimizing value of the loss function. The technique of the SA algorithm attempts to mathematically describe the process of controlled cooling associated with physical processes, the aim of which is to make the system reach the lowest value of the loss function in the face of possible local minima. The algorithm is a stochastic one that generates random states and accepts not only the "good states", which decrease the cost function (in case of minima search), but occasionally also accepts some "bad states", which increase the cost function and can help the algorithm climb out from an occasional local minimum. The basic probability distribution that governs a state's acceptance is proportional to the control parameter T, which is analogous to the temperature of a physical system, and proportional to the difference between the previous state energy J_1 and the new state energy J_2. The probability acceptance condition is $P = \exp[(J_1 - J_2)/T]$ when $(J_1 - J_2) < 0$, and 1 otherwise. The algorithm randomly chooses a control parameter and, according to the assigned temperature, changes its value. The new energy function is measured and the control parameter's new value is accepted by using the probability acceptance criterion above. Then the temperature is lowered in each step i to $T_{i+1} = \gamma T_i$, where γ is the cooling rate factor.

3. Numerical simulation of coherent beam combining using SA algorithm

3.1. System setup

The system setup for coherent beam combining of fibre amplifiers using the SA algorithm is shown in Fig. 1. The laser beam from the master oscillator (MO) is split into N channels (in the figure we show two channels as an example) and coupled to the phase modulators. The laser beams from the phase modulators (PM) are sent to optical isolator (ISO) and amplifier (AMP) and then sent to collimators (CO). It is noted that for high power application, multi-stage fibre amplifiers are often required. The beam array is sent to free space via the collimators. The collimated output beams are sampled by a beam splitter. After the splitter, part of the beam is sent to a focusing lens that images the central lobe of the far field onto a pinhole, and a detector is located immediately behind the pinhole. The opposing value of the collected power in the target pinhole is defined as the state energy J which will be used in the SA algorithm. The collected power in the target pinhole can be estimated to be equivalent to the Strehl ratio (SR),[12] so we have $J = -SR$. J is a function of the corresponding optical phase shifts $\boldsymbol{u} = (u_1, u_2, \ldots, u_N)$ added to each beamlet. The object of coherent beam combining is to minimize the state energy J (J is shared by the oscilloscope and the processor). The curve for state energy as a function of time can be shown in the oscilloscope. J is then sent into the processor through an A/D converter. The SA algorithm is performed by the processor (personal computer, the digital signal processor (DSP), can both be employed to perform the SA algorithm), corresponding optical phase shift signals are sent to the phase modulators through D/A converters. The other part of the beam after the splitter is the desired coherently combined beam array.

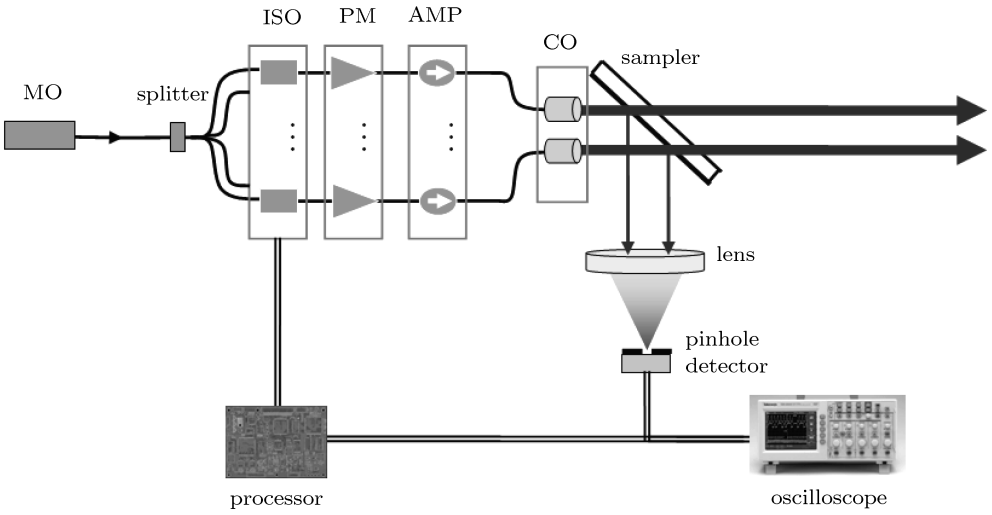


Fig. 1. System setup for coherent beam combining of fibre amplifiers using the SA algorithm.

Coherent beam combining is realized by updating the optical phase shifts in the following manner with the SA algorithm:

Step 0 Initialization: set an initial temperature T and initial parameter vector for corresponding optical phase shifts $\boldsymbol{u}^0 = \left(u_1^0, u_2^0, \ldots, u_N^0\right)$, and determine $J\left(\boldsymbol{u}^0\right)$.

Step 1 Relative to the current value $\boldsymbol{u}^m = (u_1^m, u_2^m, \ldots, u_N^m)$, randomly determine a new $\boldsymbol{u}' = (u_1', u_2', \ldots, u_N')$, and determine $J\left(\boldsymbol{u}^m + \boldsymbol{u}'\right)$.

Step 2 Compare the two J values and let $\delta = J\left(\boldsymbol{u}^m + \boldsymbol{u}'\right) - J\left(\boldsymbol{u}^m\right)$. If $\delta < 0$, then $\boldsymbol{u}^m$ is updated by $\boldsymbol{u}^{m+1} = \boldsymbol{u}^m + \boldsymbol{u}'$. Else if $\delta \geq 0$, accept $\boldsymbol{u}^{m+1} = \boldsymbol{u}^m + \boldsymbol{u}'$ only if a uniform (0,1) random variable R (generated by Monte Carlo) satisfies $R \leq \exp\left(-\delta/T\right)$, otherwise keep $\boldsymbol{u}^m$ unchanged and the control voltage is updated by $\boldsymbol{u}^{m+1} = \boldsymbol{u}^m$.

Step 3 Repeat steps 1 and 2 for some periods until either the budget of function evaluations allocated for that T has been used or the system reaches some state of equilibrium.

Step 4 Lower T according to the annealing schedule and return to step 1. Continue the process until the total budget for state energy evaluations has indicated that convergence is satisfied. Under this condition, all the laser elements are phase-locked and SR achieves its maximum value.

3.2. Static simulation

In this section, we perform feasibility validation on coherent beam combining of fibre amplifiers using the SA algorithm. Suppose that there are only static phase distortions due to the fibre optical path length differences between the different channels. Numerical calculations will be carried out to correct those phase distortions by a finite number of iterations in the SA algorithm. We will consider three square-distributed fibre laser arrays as an example. As shown in Fig. 2, all laser elements are arranged at equal-distance between elements. Figures 2(a)–2(c) denote laser arrays which contain 4, 9 and 16 lasers respectively. We suppose that each fibre laser has a single Gaussian mode output. The beam waist of each laser is ω_0. Fibre lasers are arranged in an array with the nearest neighbours separated by a distance of d. Vacancy factor $t = (d - 2\omega_0)/\omega_0$ can be used to describe the compactness of the array. A smaller t corresponds to a more compact array. The optical parameters used in calculation are as follows: $\lambda = 1.06$ μm, $\omega_0 = 5$ mm, $d = 15$ mm, $t = 1$. The far-field intensity patterns of the three laser arrays when all the laser elements are phase-locked and no phase distortions exist, are shown in Figs. 2(d)–2(f), respectively.

In the simulation, the cooling process is defined as $T_{m+1} = (\lambda)^m T_m$, where $T_0 = 10000$ and $\lambda = 0.9$. It is noted that the values of T_0 and λ will influence the converging rate of the SA algorithm. $T_0 = 10000$ and $\lambda = 0.9$ are selected to ensure the fastest converging rate from a large number of samples. We suppose the RMS value of static phase distortions in the laser array is $\sigma_p = 3\pi$ rad, which is large enough to make the beam combining almost become incoherent combining, according to the criterion proposed in Ref. [16].

The transition curves from the initial state (minimization of SR) to the desired state (maximization of SR) of the system performance are shown in Fig. 3. In this figure, the average curve over 500 transition curves is shown. From Fig. 3 one sees that the SA algorithm can converge to the extremum of the state energy for all the three laser arrays. The concept of coherent beam combining using the SA algorithm is feasible. The more lasers in the array, the more steps of iteration are required for the algorithm to converge.

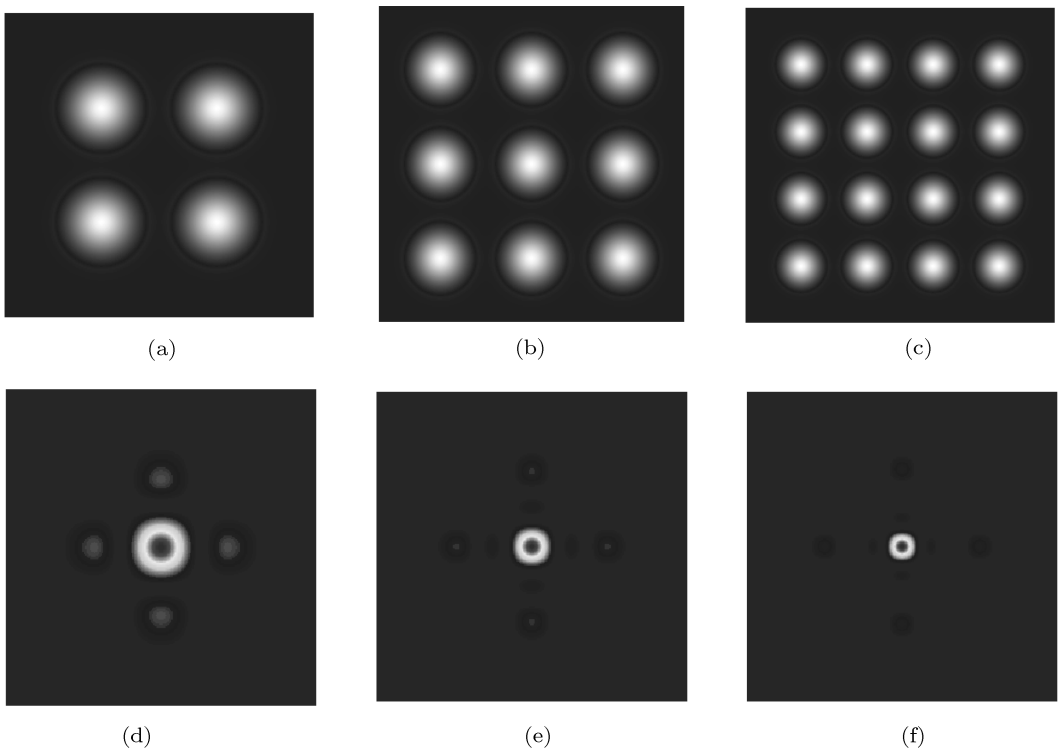


Fig. 2. Three laser arrays and their corresponding far-field intensity patterns for ideal phase-locking: (a) 4-laser array, (b) 9-laser array, (c) 16-laser array, (d) ideal far-field pattern for the 4-laser array, (e) ideal far-field pattern for the 9-laser array, (f) ideal far-field pattern for the 16-laser array.

We carry out further calculation on coherent beam combining of several other laser beam arrays (i.e., laser array contains 2, 25 and 36 lasers) using the SA algorithm. If we define the steps of iteration at which the SR value becomes larger than 0.95 as the convergence state, then the dependence of convergence rate on the number of beamlets is shown in Fig. 4. It is revealed that in coherent beam combining of N laser beamlets, the convergence rate scales at least linearly with N. This issue will bring great challenge to applying the SA algorithm to coherent combining of a relatively large number of fibre amplifiers.

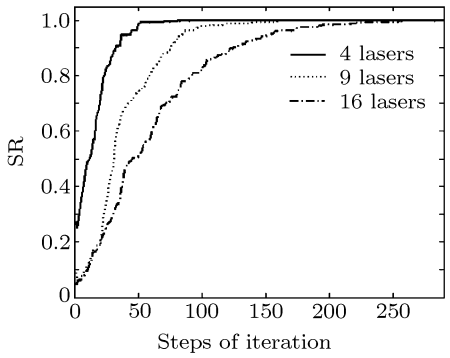


Fig. 3. Evolution curves of power in the pinhole from minimization to maximization for different laser arrays.

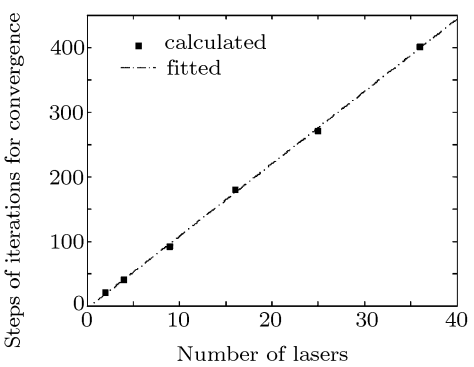


Fig. 4. The Dependence of steps required for convergence on the number of lasers for different laser arrays.

3.3. Dynamic simulation

In a practical engineering case, the phase distortions can never be static. Data on phase fluctuations has previously been reported in commercially available fibre amplifiers at power levels up to 10, 30 and 260 W.[8,17,18] It was shown that temperature variations, mechanical vibration, acoustic noise, seismic noise, etc., all can be the source for phase distortions, which cannot be avoided in practical engineering environment.

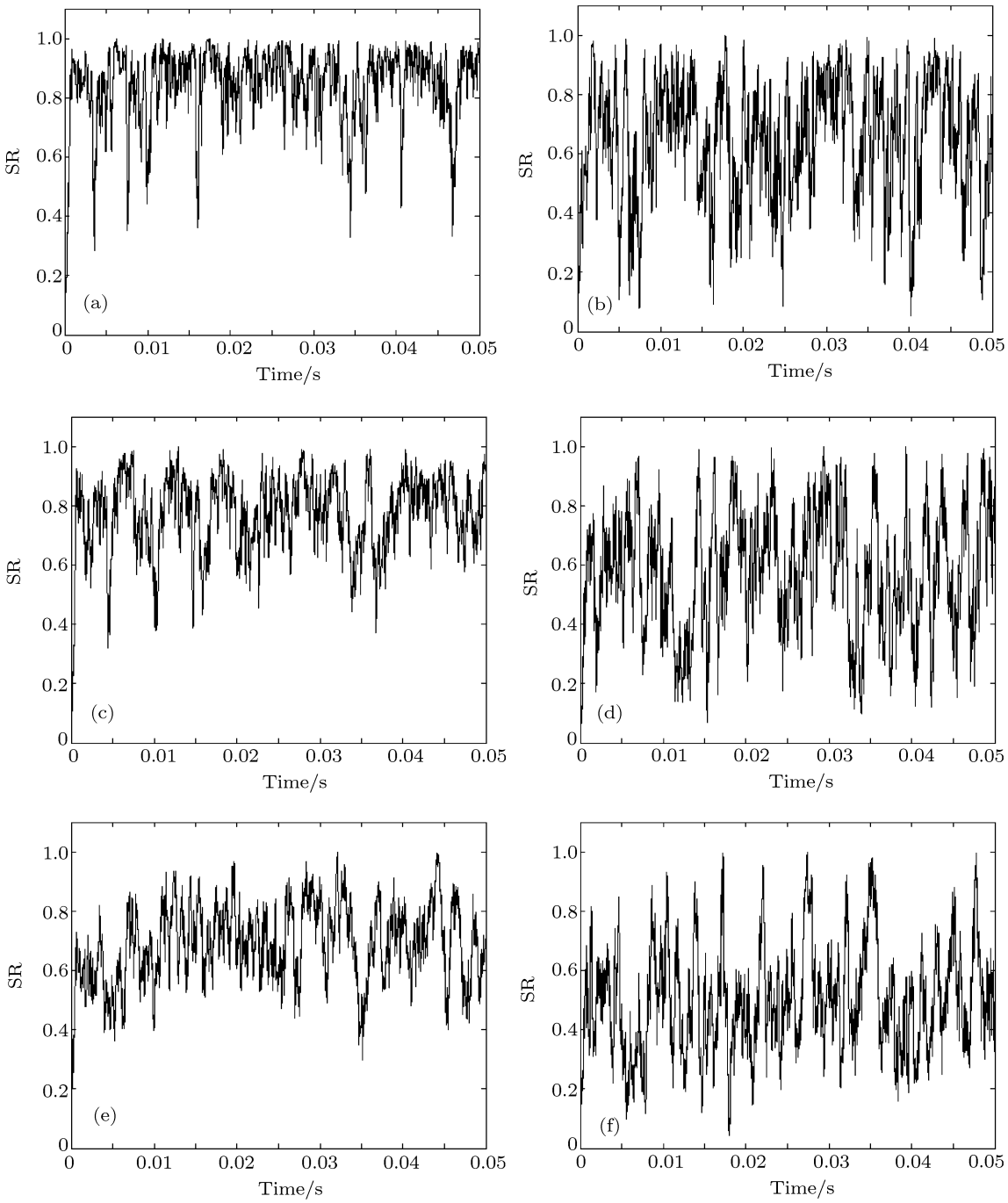


Fig. 5. Evolution curves of power in the pinhole (in time steps of 0.05 second) for different laser arrays: (a) 4-laser array, the amplitude of stochastic noise $\sigma = 0.4$ (rad); (b) 4-laser array, the amplitude of stochastic noise $\sigma = 0.6$ (rad); (c) 9-laser array, the amplitude of stochastic noise $\sigma = 0.4$ (rad); (d) 9-laser array, the amplitude of stochastic noise $\sigma = 0.6$ (rad); (e) 16-laser array, the amplitude of stochastic noise $\sigma = 0.4$ (rad); (f) 16-laser array, the amplitude of stochastic noise $\sigma = 0.6$ (rad).

In this section, we will perform dynamic simulations for coherent beam combining using the SA algorithm. Since up to date, there is no exact or even experiential mathematical model for phase distortions, we simply add stochastic noise in the process of the algorithm. At first we add stochastic noise with a bandwidth of 7 kHz[19] and different amplitude (denoted by σ) to the simulation programs to make a qualitative study on the influence of phase noise. As for the SA algorithm, we assume that the control processor can perform 100000 iterations per second (so far as we know, the most advanced microprocessor based SPGD controller can update the control voltages 95000 iterations/sec, which is demonstrated in Ref. [11]). Figure 4 shows the evolution curves of SR for a time period of 0.05 second. The numerical results show that the stochastic noise will affect the performance of coherent beam combining using the SA algorithm in two aspects. Firstly, more iteration steps will be required for the algorithm quasi-converge to the extremum of the cost function. An example is that for the 9-laser array and stochastic noise with $\sigma = 0.4$ rad amplitude, it takes more than 250 steps of iteration before SR achieves the maximum value, while for the case of no stochastic noise, only 92 steps of iteration are required, as shown in Figs. 3 and 5(c). Secondly, the SR value will never be stably controlled to the extremum due to the stochastic noise. SR will fluctuate all the time, the possibility of reaching the maximum value decreases as the amplitude of stochastic noise increases.

A further computation for studying the influence of stochastic noise with different amplitude and frequencies is carried out. The dependence of SR for different laser arrays on the frequencies of stochastic noise is plotted in Fig. 6. One sees from Fig. 6 that SR decreases with increase of the noise amplitude and frequency. In general, a laser array that contains more lasers will be affected more by the stochastic noise. It can also be concluded that the stochastic noise with amplitude larger than 2 rad will make no significant difference on the algorithm performance.

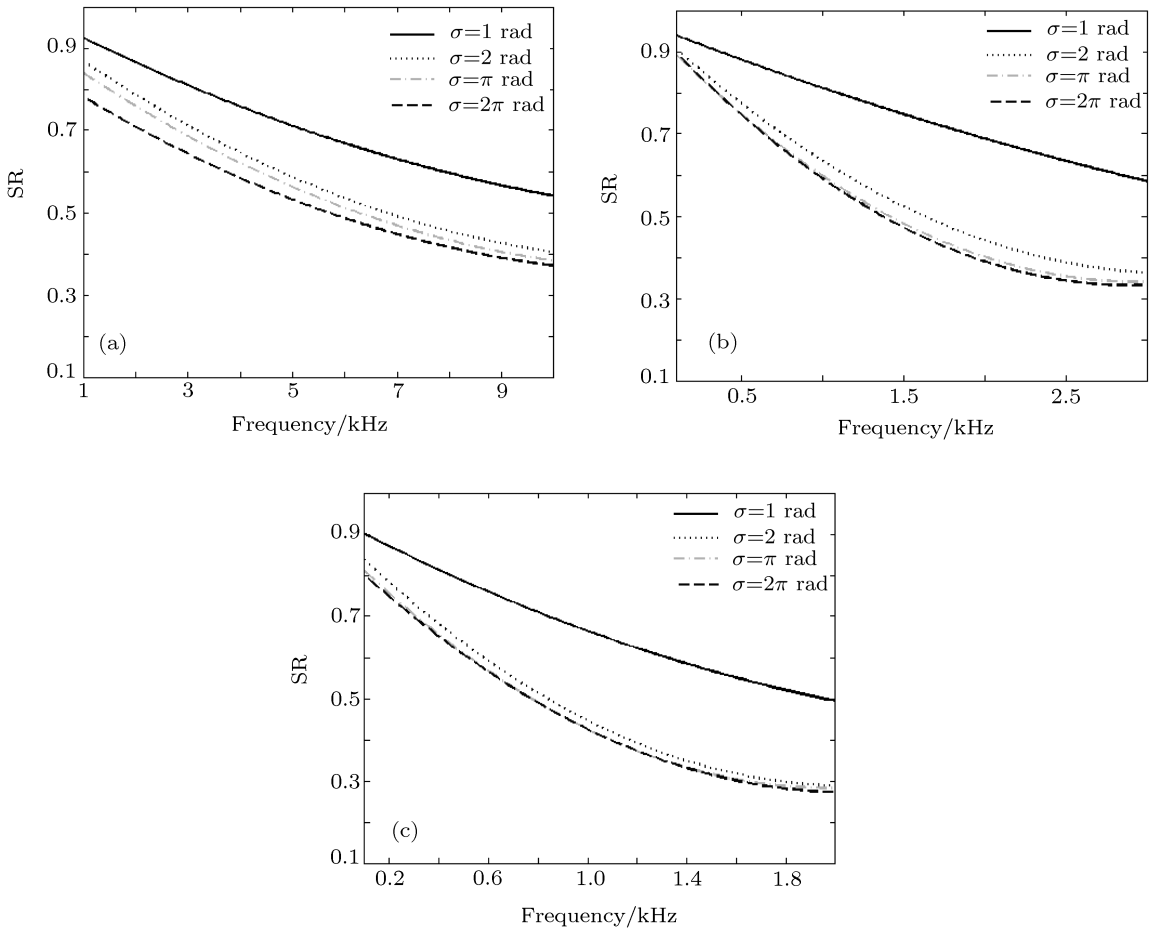


Fig. 6. Dependence of SR on the stochastic noise frequency with different amplitudes using the SA algorithm: (a) 4-laser array, (b) 9-laser array, (c) 16-laser array.

If the control bandwidth is defined as the frequency when SR equals 0.8, then the control bandwidth of SA algorithm at different noise amplitudes for different laser arrays can be computed and the result is plotted in Fig. 7. For the 16-laser array, when the periodic noise amplitudes are 1 rad and 2π rad, the control bandwidths of SA algorithm are 760 and 220 Hz, respectively. Considering that the phase fluctuates at a typical frequency of less than 100 Hz for the fibre amplifier with a 260-W output power in the laboratory environment,[18] the SA algorithm holds good in coherent beam combining of more than 10 high-power fibre amplifiers.

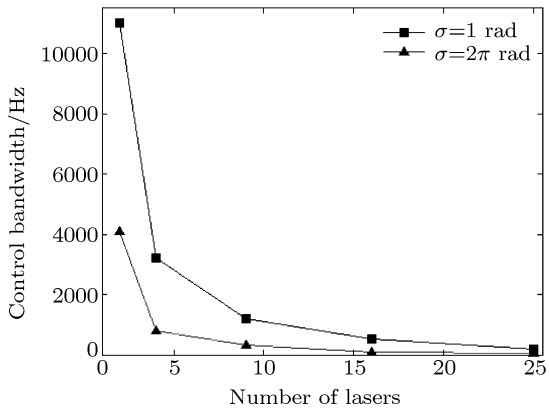


Fig. 7. Control bandwidth for different laser arrays using the SA algorithm.

4. Comparison with SPGD algorithm

SPGD algorithm has been widely used in adaptive optics fields for years,[20] and also it has been the most widely used stochastic optimization algorithm that has been applied to coherent beam combining.[2,10−12] The basic principle of standard SPGD algorithm has been detailed in formal literatures and thus it will not be repeated here. With the same parameters for the laser array and stochastic noise, the performance of standard SPGD algorithm under stochastic noise is also given. We also have to point out that in standard SPGD algorithm, three D/A and two A/D conversions are required in each iteration, while in the SA algorithm, two D/A and one A/D conversions are required, which should be taken into consideration in dynamic simulation. The dependence of SR in time steps of 0.05 second for different laser arrays on the frequency of stochastic noise using standard SPGD algorithm is plotted in Fig. 8. The control bandwidth of the two different optimization algorithms at different noise amplitudes is plotted in Fig. 9. It can be concluded from Fig. 9 that the bandwidth of SPGD algorithm is typically higher than the SA algorithm, especially at smaller noise amplitudes. This indicates that the SA algorithm is more sensitive to stochastic noise as compared with the SPGD algorithm. Nevertheless, there is no difference in magnitude; we consider that the SA algorithm also has the potential to be applied to coherent beam combining fields.

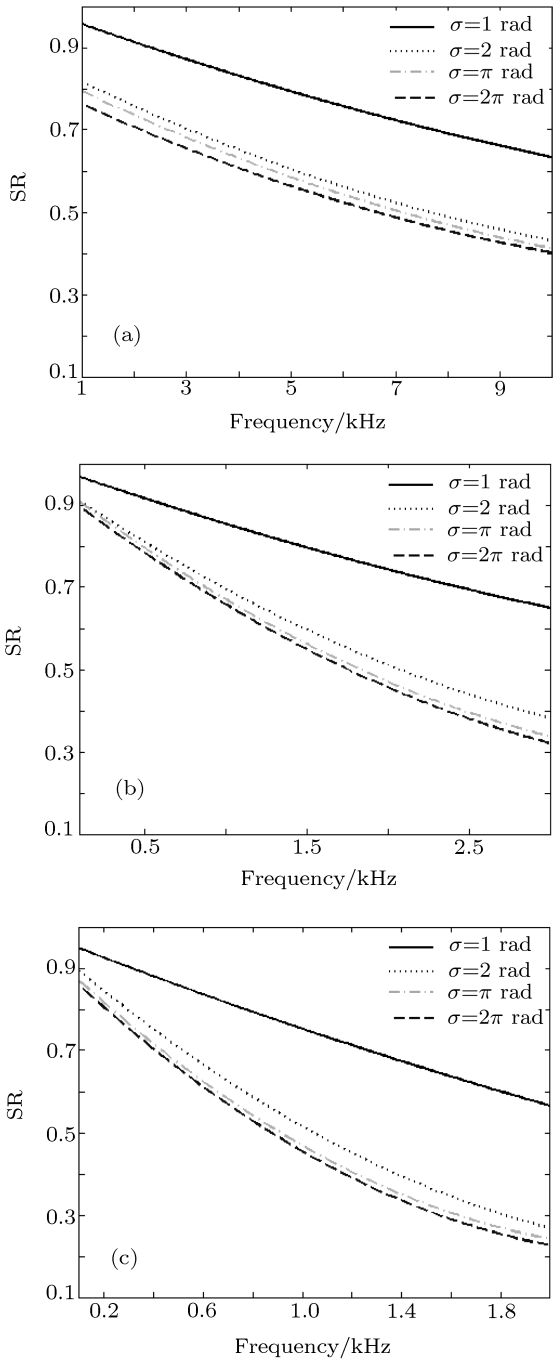


Fig. 8. Dependence of SR on the stochastic noise frequency with different amplitudes using the SPGS algorithm: (a) 4-laser array, (b) 9-laser array, (c) 16-laser array.

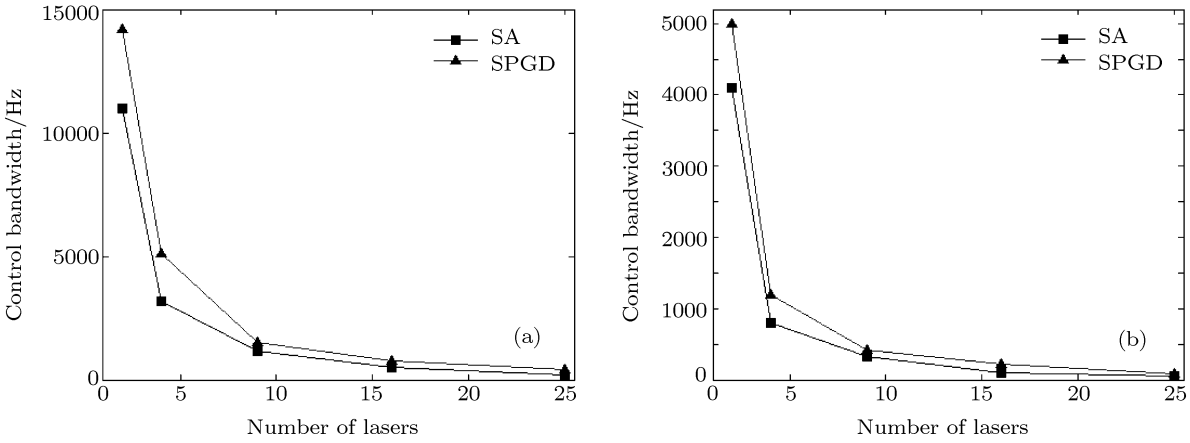


Fig. 9. Variations of control bandwidth with the number of lasers by using the SA algorithm and SPGD algorithm: (a) $\sigma = 1$ (rad), (b) $\sigma = 2\pi$ (rad).

5. Experimental results

We have performed a proof-of-concept experiment to study the coherent beam combining of two fibre amplifiers using the SA algorithm. The experimental setup is the same as that in Fig. 1. The master oscillator is a distributed feedback polarization-maintaining Yb^{3+}-doped fibre laser with a wavelength of 1083 nm and a linewidth less than 1 MHz. The laser beam from the master oscillator is split and coupled to two $LiNbO_3$ phase modulators. The distance between the centres of collimators is about 20 mm, and the beam radius of each beamlet is about 3 mm. Two stages of amplifier chains are used to boost the maximal laser output powers from the two fibre amplifiers are 5.68 W and 6.25 W, respectively. The two collimated output beams are sampled by a cubic beam splitter. After the splitter, part of the beam is sent to a focusing lens with 1 m in focusing length that images the central lobe of the far field onto a home-made pinhole with a radius of 95 μm, and a photoelectric detector is located immediately behind the pinhole. The width of the main-lobe of the far-field pattern is calculated to be 270 μm; the width of the pinhole is 35% of the main-lobe. Thus the collected power in the target pinhole can be estimated to be equivalent to the SR. The opposing value of optical signal detected is defined as the cost function J that will be used in SA algorithm. In our experiment, the SA algorithm is performed on a DSP chip and the phase controlling signal is sent to the two $LiNbO_3$ phase modulators by two D/A converters. The main frequency of the DSP chip is 25 MHz and the updating rate of control signal generated by this chip is pre-tested to be 16500 times per second. The other part of the beam after the splitter is also focused by a lens. An infrared camera is set at the focal plane to observe the far-field beam profile.

In the experiment, the optical powers of the two beamlets are both tuned to their maximal values, i.e., 5.68 W and 6.25 W. The spectral properties of fibre amplifiers are observed with an Agilent optical spectrum analyser with a resolution of 0.06 nm. Figure 10 shows the emission spectrum of one amplifier of 5.68 W output power. Amplified spontaneous emission (ASE) is suppressed by ~ 30 dB, and it has little impact on the output signal power.

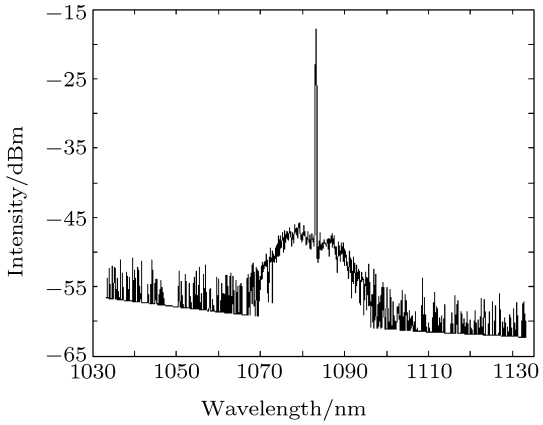


Fig. 10. Spectrum of one of the fibre amplifier.

When the SA algorithm is not implemented and the system is in open-loop, the energy contained in the target pinhole will fluctuate between 0 V and 1 V randomly. The average voltage contained in the pinhole is 0.49 V, as shown in Fig. 11(a). When the SA algorithm is implemented and the whole system is in closed-loop, the time dependence of energy contained

in the target pinhole is shown in Fig. 11(b). The cooling process is defined as $T_{m+1} = (0.9)^m T_m$, where $T_0 = 10000$. The budget of function evaluations allocated to each T is restricted to 10 times. For most of the time, the energy contained in the pinhole can be locked to nearly 1 V, which denotes the effect of coherent beam combining. The average voltage contained in the pinhole is 0.91 V when the system is in close-loop. The energy contained in the pinhole was enhanced by a factor of 1.86. The ideal effect of coherent beam combining is to enhance the energy contained in the pinhole by a factor of 2, so we can conclude that a combining efficiency of 93% is obtained.

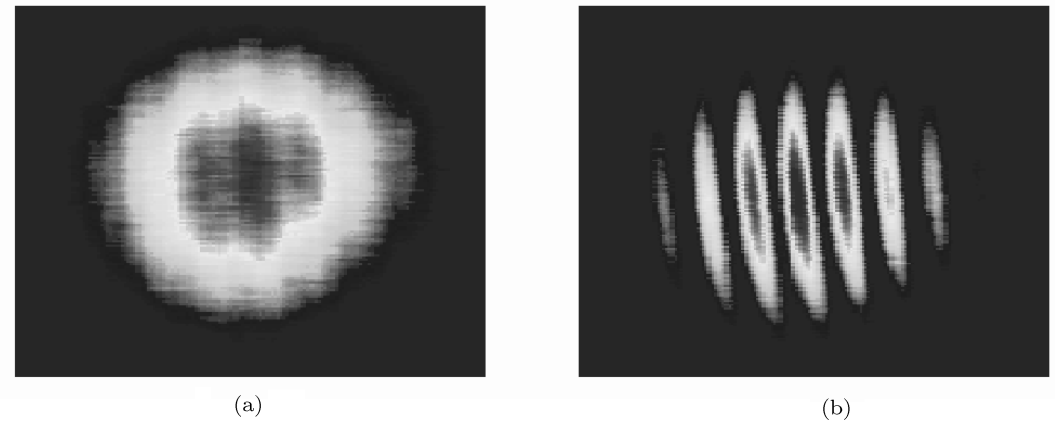


Fig. 11. Experimental results: (a) long-exposure far-field intensity distribution in open-loop, (b) long-exposure far-field intensity distribution in closed-loop.

Figure 12 shows the long-exposure far-field pattern of the combined beam when the system is in open-loop and close-loop. One sees from Fig. 11 that the visibility of the far-field fringe is remarkablely enhanced. The contrast of the far-field coherent combined beam profiles is calculated to be as high as 95%, where the fringe contrast is defined by the formula $(I_{\max} - I_{\min})/(I_{\max} + I_{\min})$, where $I_{\max}$ and $I_{\min}$ are the maximum optical intensity and the adjacent minimum on the far-field pattern, respectively.

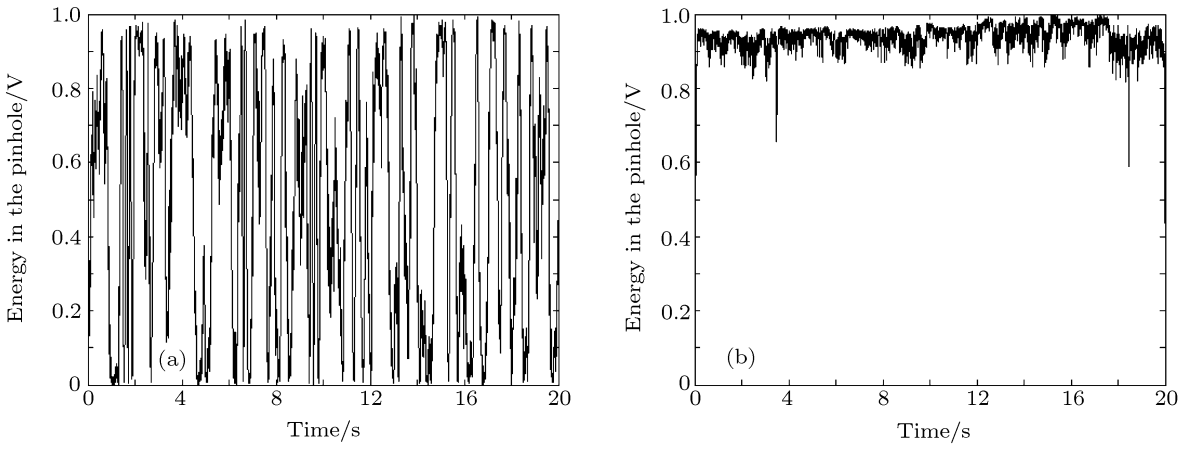


Fig. 12. Experimental results: (a) energy contained in the pinhole when the system is in open-loop, (b) energy contained in the pinhole when the system is in close-loop.

It also should be noted that the energy contained in the target pinhole will decrease to low values in intervals even in the close-loop. This can be explained as follows: On one hand, it is noted that the whole close-loop system works in an ultra-clean Laboratory, the round-the-clock working of the cooling fans at the ceiling of the room will induce high-frequency phase noise,[18] which inevitably prevents phase con-

trol based on the SA algorithm from working effectively all the time. On the other hand, in the laboratory environment, the optical phase of the laser beam may fluctuate in several hundreds of waves, thus the phase controlling signal calculated may exceed the actual range of the phase modulator, which is limited to several waves. This leads to a slight deviation in the corrected phase values and the need to reset the phase modulator.[19] The reset events cannot make the laser beams coherently combined in the intervals. Nevertheless, one sees from Figs. 11 and 12 that although high-frequency phase noise exists in the experimental environment, coherent beam combining based on the SA algorithm is relatively robust and the algorithm performs well most of the time.

6. Discussions and conclusions

We have introduced the concept of coherent beam combining of fibre amplifiers using the SA algorithm. The feasibility is validated by the Monte Carlo simulation of correcting static phase distortions. Considering the time-varying phase fluctuations in practical engineering, the performance of the SA algorithm is studied by dynamic simulation. Numerical results reveal that more steps of iteration are required for the algorithm converging into the global extremum state as compared with the static phase distortions; also in general, the influence of phase noise on the performance of the SA algorithm gets stronger as the amplitude or frequency of phase noise increases. It is also revealed that the SA algorithm is more sensitive to the stochastic noise as compared with the SPGD algorithm; nevertheless, the control bandwidths of these two algorithms do not have a difference in magnitude. A proof-of-concept experiment is performed to demonstrate that the SA algorithm is feasible in a coherent beam combining field.

Numerical results also indicate that a laser array composed of more lasers will suffer more from phase noise. This should be considered when coherent combining includes a relatively large number of lasers. We think that this issue can be solved in two aspects. First, more advanced controllers that have a faster updating rate should be investigated, and secondly, corresponding countermeasures should be taken to suppress the influence of phase noise. This contains technical details in practical engineering, which is beyond the scope of this paper, so we do not go into it here. The simulation study performed in this paper can be helpful for designing and analysing an experimental system for coherent beam combining using the SA algorithm.

References

[1] Fan T Y 2005 *IEEE J. Sel. Top. Quantum Electron.* **11** 567

[2] Shay T M, Baker J T, Sanchez A D, Robin C A, Vergien L C L, Zerinque C, Gallant D, Lu C A, Pulford B, Bronder T J and Lucero A 2009 *Proc. SPIE.* **7195** 71951M-1

[3] He B, Lou Q H, Zhou J, Dong J X, Wei Y R, Xue D, Qi Y F, Su Z F, Li L B and Zhang F P 2006 *Opt. Express* **14** 2721

[4] Xiao R, Hou J and Jiang Z F 2006 *Acta Phys. Sin.* **55** 6464 (in Chinese)

[5] Chen Z L, Hou J, Zhou P and Jiang Z F 2007 *Acta Phys. Sin.* **56** 7046 (in Chinese)

[6] Wang J M, Duan K L and Wang Y S 2008 *Acta Phys. Sin.* **57** 5627 (in Chinese)

[7] Peng Q, Zhou Y, Chen Y, Sun Z, Bo Y, Yang X, Xu Z, Wang Y, Li K and Zhao W 2005 *Electron. Lett.* **41** 171

[8] Cheng Y, Liu Y, Xu L and Zheng R 2009 *Chinese Journal of Lasers* **36** 77 (in Chinese)

[9] Jia X J, Liu F N, Fu S G, Liu Y G, Yuan S G and Dong X Y 2007 *Chin. Phys.* **16** 2993

[10] Liu L, Vorontsov M A, Polnau E, Weyrauch T and Beresnev L A 2007 *Proc. SPIE.* **6708** 67080K-1

[11] Kansky J E, Yu C X, Murphy D V, Murphy D V, Shaw S E J, Lawrence R C and Higgs C 2006 *Proc. SPIE.* **6306** 63060G-1

[12] Zhou P, Liu Z J, Wang X L, Ma Y X, Ma H T, Xu X J and Guo S F 2009 *J. Sel. Topics Quantum Electron.* **15** 248

[13] Ribak E N, Alder J and Lipson S G 1990 *J. Phys.* A **23** L809

[14] Zommer S, Ribak E N, Lipson S G and Alder J 2006 *Opt. Lett.* **31** 1

[15] Spall J C 2003 *Introduction to Stochastic Search and Optimization* (New Jersey: John Wiley & Sons) p. 208

[16] Nabors C D 1994 *Appl. Opt.* **33** 2284

[17] Augst S J, Ranka J K, Fan T Y and Sanchez A 2007 *J. Opt. Soc. Am.* B **24** 1707

[18] Jones D C, Stacey C D and Scott A M 2007 *Opt. Lett.* **32** 466

[19] Tröbs M, Wessels P and Fallnich C 2005 *Opt. Lett.* **30** 789

[20] Vorontsov M A, Carhart G W and Cohen M 2000 *J. Opt. Soc. Am.* A **17** 1440